Available online at www.sciencedirect.com
ScienceDirect
Journal of Power Sources 177 (2008) 652–659
JOURNAL OF POWER SOURCES
www.elsevier.com/locate/jpowsour

Solid state double layer capacitor based on a polyether polymer electrolyte blend and nanostructured carbon black electrode composites

Rodrigo L. Lavall [a], Raquel S. Borges [a], Hállen D.R. Calado [a], Cezar Welter [a], João P.C. Trigueiro [a], Jacques Rieumont [a,b], Bernardo R.A. Neves [c], Glaura G. Silva [a,*]

[a] *Departamento de Química, Instituto de Ciências Exatas, Universidade Federal de Minas Gerais, CEP 31270-901, Belo Horizonte, Brazil*
[b] *Facultad de Química, Universidad de La Habana, Habana 10400, Cuba*
[c] *Departamento de Física, Instituto de Ciências Exatas, Universidade Federal de Minas Gerais, CEP 31270-901, Belo Horizonte, Brazil*

Received 22 August 2007; received in revised form 9 November 2007; accepted 12 November 2007
Available online 26 November 2007

Abstract

An all solid double layer capacitor was assembled by using poly(ethylene oxide)/poly(propylene glycol)-*b*-poly(ethylene glycol)-*b*-poly(propylene glycol)-bis(2-aminopropyl ether) blend (PEO-NPPP) and $LiClO_4$ as polymer electrolyte layer and PEO-NPPP–carbon black (CB) as electrode film. High molecular weight PEO and the block copolymer NPPP with molecular mass of 2000 Da were employed, which means that the design is safe from the point of view of solvent or plasticizer leakage and thus, a separator is not necessary. Highly conductive with large surface area nanostructured carbon black was dispersed in the polymer blend to produce the electrode composite. The electrolyte and electrode multilayers prepared by spray were studied by differential scanning calorimetry, atomic force microscopy (AFM) and impedance spectroscopy. The ionic conductivity as a function of temperature was fitted with the Williams–Landel–Ferry equation, which indicates a conductivity mechanism typical of solid polymer electrolyte. AFM images of the nanocomposite electrode showed carbon black particles of approximately 60 nm in size well distributed in a semicrystalline and porous polymer blend coating. The solid double layer capacitor with 10 wt.% CB was designed with final thickness of approximately 130 μm and delivered a capacitance of 17 F g^{-1} with a cyclability of more than 1000 cycles. These characteristics make possible the construction of a miniature device in complete solid state which will avoid electrolyte leakage and present a performance superior to other similar electric double layer capacitors (EDLCs) presented in literature, as assessed in specific capacitance by total carbon mass.

Keywords: Solid double layer capacitor; Polymer electrolyte blend; Composite electrode; Nanostructured carbon black

1. Introduction

The increased use of portable electronic equipments such as mobile telephones, laptops, etc. as well as power supply demands for electric vehicles have been generating a great effort in the investigation of new alternatives for performance improvement of batteries, fuel cells and capacitors [1–5]. Additionally, the design of miniaturized and safe components continues to be a challenge in the area [6]. Electrochemical capacitors using the charge of the electric double layer at the electrode/electrolyte interface of a highly porous electrode coupled with polymer electrolyte films can have an important role in new technologies.

Carbon-based materials have been widely used in electrodes for electric double layer capacitor (EDLC), where the relationships between the surface area, total pore volume, average pore size and the pore size distribution have strong influence in the electrochemical characteristics of the capacitor [7]. In such devices, activated carbon, carbon black (CB) or carbon nanotube composites have been applied as electrodes [4,8,9] mainly by using liquid electrolytes [10]. The use of solid polymer electrolytes (SPE) has been much more restricted [5,11–18]. Usually, the electrolytes employed in the electrochemical capacitors are

* Corresponding author. Tel.: +55 31 34995768; fax: +55 31 34995700.
E-mail addresses: rllavall@yahoo.com.br (R.L. Lavall), raquel-sb@uol.com.br (R.S. Borges), hallendaniel@yahoo.com.br (H.D.R. Calado), cwelter@fisica.ufmg.br (C. Welter), joaopcampos@yahoo.com.br (J.P.C. Trigueiro), jacques@fq.uh.cu (J. Rieumont), bernardo@fisica.ufmg.br (B.R.A. Neves), glaura@qui.ufmg.br (G.G. Silva).

0378-7753/$ – see front matter © 2007 Elsevier B.V. All rights reserved.
doi:10.1016/j.jpowsour.2007.11.060

acids, bases or salts dissolved in aqueous or organic solvents. The utilization of corrosive liquid electrolytes may be the cause of dangerous leakage that decreases the safety and the lifetime of the capacitors [6,16]. A way to reduce these problems associated with the management of corrosive ionic conductors, as well to the preparation of thin film cells with high reliability, is the use of solid polymer electrolyte [14,16]. The most promising materials for solid polymer electrolytes are based on poly(ethylene oxide) (PEO), but the high crystallinity of PEO has been a drawback for its use as SPE [19]. Blending two polymers is one of the procedures that may contribute to overcome these problems [20].

The low conductivity of SPEs is the main limitation for their use as electrolyte in power devices. However, the improved properties of new carbon materials and a careful design of the polymer electrolyte can produce enhancement in the characteristics of a solid polymer EDLC in such a way that it becomes competitive in some practical aspects. For example, safety concerns are driving high interest to the research and development of solid polymer-based EDLC and the processing of thin plastic films can produce an increase in the power by volume of the device.

In order to take into account the problem of low conductivity in polymer electrolyte samples, it is necessary to persist in the investigation of the conductivity behavior as a function of composition and temperature. The aim here is to look for insights that may introduce gains of conductivity in specific experimental conditions. The conductivity changes of solid polymer electrolytes with temperature have been studied for almost three decades with different formalisms such as the Vogel–Tamman–Fulcher (VTF) and Williams–Landel–Ferry (WLF) [21–28]. WLF is more universal for glasses and polymers and, moreover, good linear correlations between conductivity and viscosity [21] and ^{7}Li NMR line width [25] have been obtained and successfully described by WLF for polymer metal–ion complexes. Experimental data indicate that other complex patterns can be obtained for SPEs, such as Arrhenius behavior at low temperature and WLF at high temperatures, or Arrhenius with two different activation energies [26,27]. One of the problems of these approaches is the temperature dependence of their parameters, in particular on the temperature interval used [29], as well as its interpretation [30].

Carbon black is a particulate form of carbon produced by processes that involve thermal decomposition or partial oxidation of hydrocarbon materials [31]. In these processes, layer structures composed of hexagonal carbon rings are formed. These structures tend to stack in three to four layers forming crystallites whose specific organization leads to the formation of primary particles, which further fuse into nanosized primary aggregates [9,32]. These aggregates, due to van der Waals forces, join together in more loosely assembled agglomerates. The aggregate size and shape and the number of particles per aggregate determines the structure of carbon black. Depending on the preparation procedure, carbon black has the advantage that it can be obtained in a range of diameter from 10 nm to 100 nm, forming extremely porous materials with large surface areas (100–2000 $m^2\,g^{-1}$) [9,31,32]. CB has been chosen as filler for conducting rubbers and conducting plastics because of their low cost, low density, high electrical conductivity and specific structures that enable a formation of conductive network inside a polymer matrix at relatively low filler concentration [33]. However, only carbon blacks with small diameter and large surface area are suitable as the filler to improve electric conductivity [32]. Black Pearls 2000 (Cabot) fulfills these requirements: it possess a BET surface area of 1500 $m^2\,g^{-1}$, a particle size of 12 nm and a highly aggregated structure, which leads to the formation of conductive pathway, allowing to achieve a continuous electron flow through polymeric composites (lowering the resistivity) [31], at relatively low concentration of the filler (low percolation threshold).

Our group has previously reported the study of materials for electrochemical capacitors using CB and PEO mixed with PEG (molecular weight 400) as plasticizer [5] or an aliphatic thermoplastic polyurethane with a polyether segment of molecular weight 800 [11], both materials were prepared by conventional casting technique. Further improvement is presented here by developing electrolyte and electrode films prepared by spray coating and the assembly of a capacitor built on the basis of the nanostructured carbon black composite electrode (CE) with a solid polymer electrolyte blend (SPEB)—using polyethers as matrix and $LiClO_4$ as the ion source. The low molecular weight triblock polyether was blended with PEO in order to improve both electrolyte and electrode performances, leading to (i) increased ionic conductivity of the SPE, (ii) increased wettability of CB in the electrode, (iii) maintenance of dimensional and electrochemical stability of SPE and CE, and (iv) enhancement of ion access to CB pores.

2. Experimental

Materials used to prepare polymer electrolytes SPE and composite electrodes by spray casting were the following: poly(ethylene oxide) (Aldrich Mw 100,000 g mol^{-1}, supplier data), $LiClO_4$ (Aldrich), poly(propylene glycol)-*b*-poly (ethylene glycol)-*b*-poly(propylene glycol)-bis(2-aminopropyl ether) (NPPP) (Aldrich, Mn = 2000 g mol^{-1}, supplier data), carbon black (Cabot, Black Pearls 2000, 1500 $m^2\,g^{-1}$, supplier data) and tetrahydrofuran (THF) (Synth). All reagents were used as received.

The electrolyte blends were prepared with 20 wt.% of the block copolymer with respect to the PEO and 18 wt.% $LiClO_4$ [34] in two different ways: (i) PEO and NPPP were dissolved together with THF under magnetic agitation. After solubilization of polymers, the salt was mixed under agitation to produce the electrolyte PE1, and (ii) each polymer was solubilized separately in THF and the salt was added to the flask with NPPP under agitation. After the complete solubilization, the two solutions were mixed to produce the electrolyte PE2. For comparison, a blend (BLD) with 20 wt.% of the block copolymer with respect to the PEO was prepared (in the same way of PE1) without salt addition.

The specific superficial area of the carbon black was investigated by using the Brunauer-Emmett-Teller (BET) method, with the data of N_2 adsorption/desorption with Quantachrome

Autosorb Automated Gas Sorption System NOVA 1200. The specific superficial area for CB was determined as 1680 $m^2\ g^{-1}$. This value is in agreement with the supplier data and very close to the values obtained by other groups for the same commercial sample from Cabot [35]. The isotherm (not shown) indicated the presence of micropores (<2 nm) and mesopores (2–50 nm). The X-ray diffraction measurements of the CB, obtained with a Rigaku diffractometer model Geigenflex, with a cobalt Kα (λ = 1.790 Å) source with angular diffraction 2θ scanning in the interval between 4° and 70°, showed broad signals close to 2θ 27.2° and 50.3°, which indicate the presence of small graphite crystals [36].

The composite electrodes were prepared using a blend of PEO and 20 wt.% of NPPP as polymeric matrix. In the composite electrodes, named CE5 and CE10, 5 wt.% and 10 wt.% of carbon black were used as filler. No salt was used in the electrodes in order to prepare coatings with good dimensional stability. After preparation, the suspensions for electrode samples were sonicated (in a low power ultrasonic bath) for 5 h to produce a high dispersion of CB in the polymer.

The solutions/suspensions were sprayed on stainless steel substrates. The solvent evaporation was carried out in an oven under vacuum at 90 °C during 24 h. After that, the temperature control was turned off and the films were kept in the oven to reach the ambient temperature and then rapidly transferred to a desiccator and maintained under vacuum.

Modulated DSC was carried out with a TA Instruments 2920 DSC, in six scanning experiments, three heating stages and three cooling stages, between −120 °C and 120 °C at heating rate of 10 °C min^{-1}, under He atmosphere (50 mL min^{-1}) in order to evaluate the influence of possible residual solvent or adsorbed humidity in the thermal properties of the materials and to assess differences between fast and slow crystallization/melting behaviors. The second DSC heat scanning was used to determine phase transitions, and the third DSC heat scanning confirmed the results obtained on the second one.

Electrical measurements were performed with an Eco Chemie potentiostat/impedance frequency analyzer Autolab PGSTAT 30. An experimental cell including two stainless steel disk electrodes (collectors) was used for the measurements of the conductivity of electrolytes and composite electrodes in the range of temperature from 25 °C to 95 °C. The measurements were accomplished at least in triplicate in the frequency range from 0.5 Hz to 5×10^5 Hz with 50 mV amplitude.

For the capacitor analysis, complete cells were made by preparing two elements consisting of C:CE configuration (C = collector) and then set up to sandwich a SPE film under a low pressure. The electrochemical and AC electrical properties were characterized at room temperature also at least in triplicate. The frequency ranged from 1×10^{-3} Hz to 1×10^6 Hz at 0 V with 50 mV amplitude for the impedance measurements. The electrical parameters were deduced using an equivalent circuit program, EQUIVCRT (B.A. Boukamp) or free Zview version 2.8d (demonstration mode) from Scribner Associates Inc. written by Derek Johnson.

Cyclic voltammetry (CV) for the EDLC was carried out in the voltage range from −1.0 V to +1.4 V at 5 mV s^{-1}. The CV curves were fitted with equation corresponding to the current response to a linear potential scanning:

$$i(t) = +vC(1 - e^{-(t-\tau)/RC}) + i(\tau)\, e^{-(t-\tau)/RC} + \frac{V}{R+r} \qquad (1)$$

where i is the current (A), v the scan rate (V s^{-1}), C the capacitance (F), R the resistance (Ω), t the time (s), τ the time of the scan rate inversion (s), V is potential at each point and r is an ohmic resistance as shown in Figure 3 of Ref. [7]. The fitting procedure provided values of resistance and capacitance. Chronocoulometry measurements were carried out with the complete cell charged/discharged by applying, respectively, 1 V for 5 min and −1 V for 5 min. Capacitance determination was accomplished through the use of $C = dQ/dV$, with the charge value after 5 min and potential of 2 V (the difference between +1 V and −1 V).

The thickness of the layers was determined by using a Mitutoyo digital micrometer with 1 μm of precision under a table of measurement of high accuracy. The electrolyte and electrode thicknesses were characterized between 10 μm and 30 μm.

The surface of the samples was observed in an Olympus BX 50 optical microscope, which allowed a first evaluation of the coating quality and selection of samples. A Jeol JSM 840A electron microprobe (EDS = energy dispersive X-ray and WDS = wavelength dispersive spectrometer) was used to assess the degree of dispersion of carbon black on the film. Atomic force microscopy images were obtained with a Veeco Instruments MultiMode SPM with a Nanoscope IV controller. For such images, sample films were prepared in a Si substrate.

3. Results and discussion

3.1. The solid polymer electrolyte blend

Fig. 1 shows the DSC second heating scan curves obtained for the two electrolytes and two electrodes films. The main thermal properties are summarized in Table 1, which includes thermal data for the pure polymers and the blend between them. Table 1

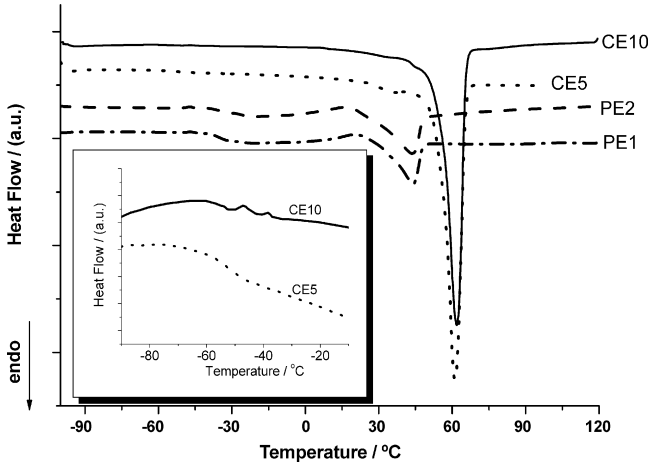

Fig. 1. DSC curves for the electrolytes and electrodes. PE1 and PE2 were prepared with a PEO/NPPP blend and 18 wt.% of $LiClO_4$ by two slightly different procedures. CE5 and CE10 are based on carbon black added to the polymer blend (5 wt.% and 10 wt.%) without salt.

Table 1
Main thermal data (from DSC curves) for the two polymeric matrices, the blend without salt (BLD), the electrolytes (PE1 and PE2) and the carbon black-based composites (CE5 and CE10)

Sample	T_g (mid point) (°C)	T_c (peak) (°C)	ΔH_c (J g^{-1})	T_m (peak) (°C)	ΔH_m (J g^{-1})
PEO	−57	–	–	62	122
NPPP	−53	–	–	37/46[a]	127
BLD	−52	–	–	61	125
PE1	−35	21	10	44	21
PE2	−35	17	11	44	23
CE5	−53	–	–	61	119
CE10	−53	–	–	62	116

[a] Main peak with a shoulder.

shows that both PE1 and PE2 electrolytes are quite similar. The preparation procedure is different in the sense that the salt was added first on the triblock when preparing PE2. This was accomplished to test the possibility of preferential solvation by one of the polymers of the blend. Therefore, from the point of view of their thermal properties, both polymer electrolyte samples have similar polymer-salt structure. The single T_g found for these two electrolytes confirm the miscibility of PEO and NPPP components. Actually, this compatibility is already verified in the blend were no salt is present and a single T_g is observed at −52 °C. In both electrolytes, the addition of salt to the blend produced the decrease of the main melting transition to 44 °C, with an abrupt decrease in heat of fusion, and an increase of the glass transition to −35 °C. This is a typical result for an electrolyte system where lithium cations coordinate with ethylene oxide units leading to the formation of a more rigid amorphous structure with concurrent strong decrease in crystallinity [19,28]. A fast ionic transport is reported to take place in the amorphous regions of the electrolyte when it is semicrystalline [37,38]. Thus, the observed decrease of crystallinity is an important factor to improve conductivity in the class of SPE employed in this work.

The study of conductivity as a function of temperature was performed on cooling after a first heating to 100 °C to minimize possible deviations in the conductivity due to solvent residues or defective electrolyte/electrode contact. The Arrhenius plot presented in Fig. 2 shows that for both electrolytes the conductivity varied from 10^{-5} S cm^{-1} to 10^{-3} S cm^{-1} in the temperature range between 25 °C and 100 °C. The differences in conductivity between PE1 and PE2 observed in Fig. 2 can be considered within the intrinsic error of the measurement. Therefore, the different preparation procedures did not induce any significant changes in the conductivity behavior, which is in agreement with the thermal results.

The temperature dependence of ionic conductivity for the completely amorphous PEO–lithium salt complexes shows a continuously curved profile that can be described by the free volume-based equations such as WLF [24,39,40]. The conductivity trend of the solid polymer electrolyte blends has been analyzed by using the WLF equation choosing T_g as T_{ref} in the logarithmic plot of log σ versus $(T - T_{ref})^{-1}$. The logarithmic plots for the electrolytes in the present work did not allow good adjustments in both cases, which can be considered to be associated to the semicrystalline nature of the SPE and the limited range of temperature in the measurement. However, Watanabe et al. [24] previously calculated the values of the C_1 and C_2 constants with the WLF equation for semicrystalline systems. Therefore, further attempts to obtain those values were conducted by using the linear form of WLF equation for conductivity [24,25]:

$$\frac{1}{\ln(\sigma/\sigma_g)} = \frac{1}{C_1} + \frac{C_2}{C_1(T - T_g)}, \quad \text{at } T_g \tag{2}$$

or

$$\frac{1}{\ln(\sigma/\sigma_{ref})} = \frac{1}{C_1'} + \frac{C_2'}{C_1'(T - T_{ref})}, \quad \text{at } T_{ref} \neq T_g \tag{3}$$

Because the conductivity data close to T_g could not be measured in this work, another reference temperature was selected (T_{ref} = 25 °C). Then, the original constants C_1 and C_2 can be estimated using the following relations, as already reported [24]:

$$C_1 = \frac{C_1' C_2'}{C_2' - (T_{ref} - T_g)} \tag{4}$$

and

$$C_2 = C_2' - (T_{ref} - T_g) \tag{5}$$

Values of C_1 equal to 23.6 and C_2 of 45.7 were obtained for the electrolyte PE1. These values are different from the values originally reported in the paper of WLF (C_1 = 17.4 and

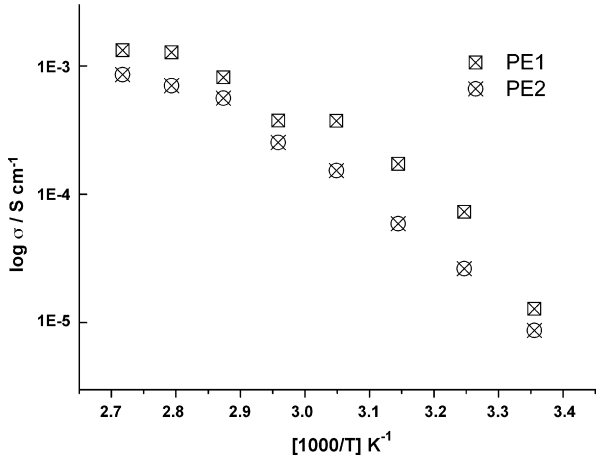

Fig. 2. Arrhenius plot for the electrolytes based on PEO-NPPP/$LiClO_4$. Two samples PE1 and PE2 prepared with different procedures.

$C_2 = 51.6$) [41], which can be related to the fact that the systems are semicrystalline, as previously discussed by Watanabe et al. [24]. The C_2 value obtained in the present work is in the range observed for partially crystalline PEO-based network with LiBr salt electrolyte [24].

The previous discussion is important because the conductivity mechanism is typical of a solid homogeneous polyether-based SPE, even considering the content of a low molecular weight component in the blend. The values of conductivity were on the range of amorphous SPE, but there is room for further enhancement by adding a higher amount of NPPP.

3.2. The composite electrodes

The blend PEO-NPPP was used to prepare the composite electrodes with carbon black nanoparticles. The electrodes were prepared with CB concentration of 5 wt.% and 10 wt.%. The conductive theoretical percolation threshold for spherical particles is 16 vol%. However, CB can be considered as particles of aspect ratio close to 10 because the primary agglomerates, which are present in the composites, are extended in one direction [42]. In the case of randomly dispersed cylinders with aspect ratio equal to 10, the theoretical percolation threshold is 12 vol% [43]. Therefore, the carbon black fluffy aggregates used in this work were added in concentrations of 5 wt.% and 10 wt.% in the CE based on these previous assumptions. It is noticeable that a higher concentration could provide higher conductivity and mainly, an enhanced capacitance for the device. However, the dispersability is compromised and the aggregate size increases. Moreover, the wettability of CB surface may be severely compromised in a totally solid system if the particles are not well dispersed. Thus, a balance between these factors should be pursued.

WDS carbon maps and EDS analysis in at least three different points of the surface (not shown) indicated that the CB is distributed quite homogeneously in a micrometric scale throughout the whole film surface. Details of the surface can be observed in the AFM phase contrast images presented in Fig. 3. The carbon black particles are incrusted in the polymer lamellae. DSC experiments reveal no significant differences between heat of melting for PEO, NPPP, blend and the composites as shown in Table 1. The data from DSC curves shows that the carbon black presence does not cause pronounced change in the phase arrangement of the matrix, which is in agreement with the AFM images.

The size distribution of CB aggregates was assessed from 20 different particles in two different regions observed in AFM images with higher magnification for each composition. The obtained average diameter was 60–70 nm for both the 5 wt.% and 10 wt.% CB nanocomposites, without significant differences between them.

The conductive behavior was investigated by impedance spectroscopy in the temperature range between 25 °C and 95 °C. Conductivity data for the two composite samples show constant values with temperature in the order of 10^{-6} S cm^{-1} for electrodes with 10 wt.% of CB and 10^{-5} S cm^{-1} for electrodes with

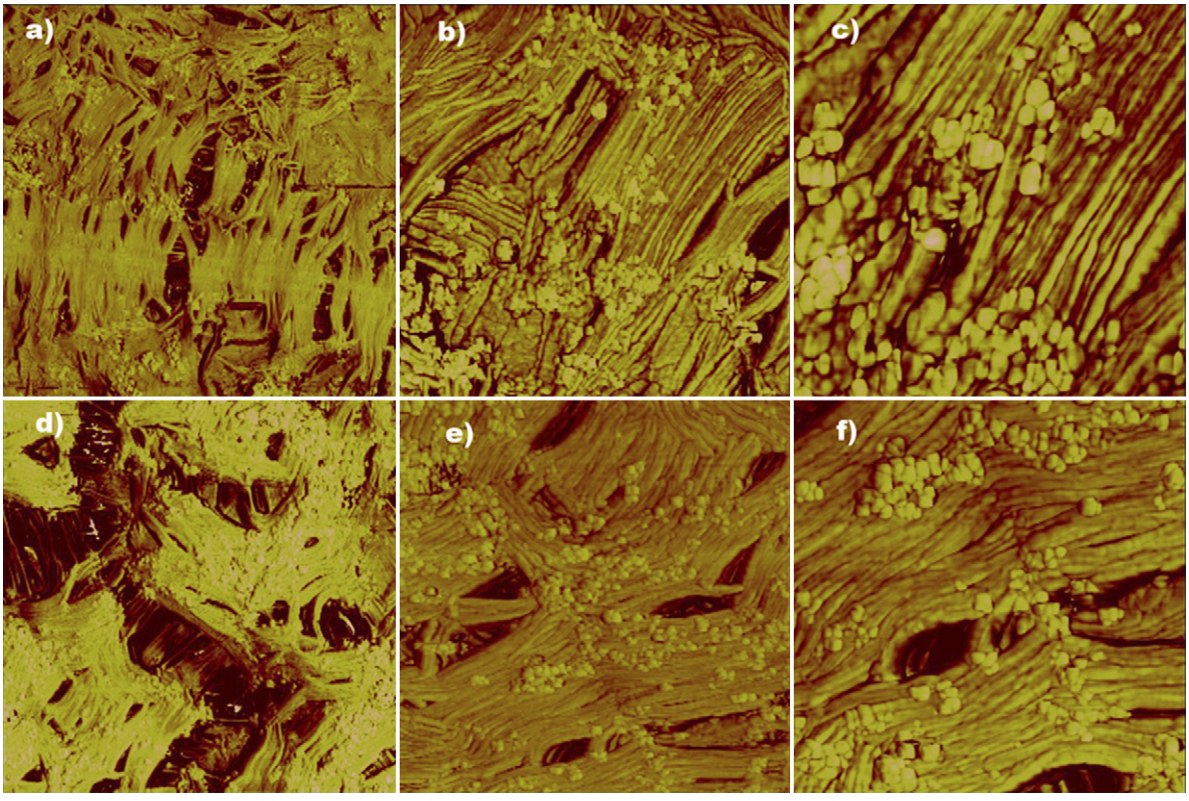

Fig. 3. AFM phase contrast image for polymer blend composite with 5 wt.% CB at magnifications of total width: (a) 10 μm, (b) 3 μm and (c) 1.2 μm, and for 10 wt.% CB at magnifications of total width: (d) 8 μm, (e) 3 μm and (f) 2 μm.

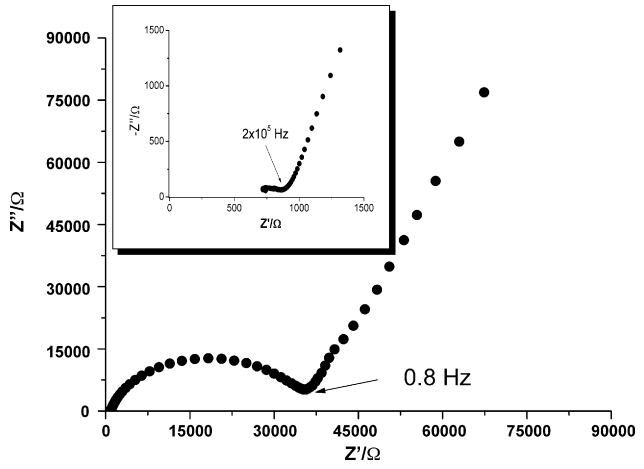

Fig. 4. Impedance spectra for the EDLC with 5 wt.% CB in the 1×10^{-3} Hz to 1×10^{6} Hz frequency range with 50 mV amplitude.

5 wt.% of CB, which could be related to inter-particle separation by insulating polymer and the highly porous and crystalline structure of the matrix, as can be observed in Fig. 3 and Table 1. The isolated composite electrode conductivity is certainly quite small. However, taken into account that these composite films are micrometric and highly porous, the spray of the polymer electrolyte solution over the CE will impregnate the coating with the electrolyte and will allow the ionic species to diffuse to regions inside the composite film, reaching the CB aggregates. This possibility leads to interesting results, on the complete device, which will be presented in the next section.

3.3. The device

Double layer capacitors with 5 wt.% and 10 wt.% CB were set up by sandwiching a micrometric coating of SPEB between also micrometric coatings of the nanocomposite electrodes. Typically, the device was designed with two electrodes of ~30 μm thickness, electrolyte of ~70 μm thickness and area of 1.26 cm^2. The solid electrolyte film guarantees the separation between the electrodes. The complete impedance response of the capacitor CB(PEO-NPPP)/(PEO-NPPP–$LiClO_4$)/CB(PEO-NPPP) with 5 wt.% CB content electrodes is shown in Fig. 4. As discussed previously [11], the high frequency pseudo semi-circle, characterized in the range of frequency shown in Fig. 4 inset, is associated to the resistive and capacitive behavior of PE bulk. The second semi-circle at intermediate frequencies and fully observed in Fig. 4 is assigned to the inter-aggregate impedance within CE. At low frequency, the quasi 90° phase shift response is assigned to the double layer capacitance of carbon/electrolyte interface. The data of capacitance obtained for the devices with 5 wt.% and 10 wt.% CB are summarized in Table 2.

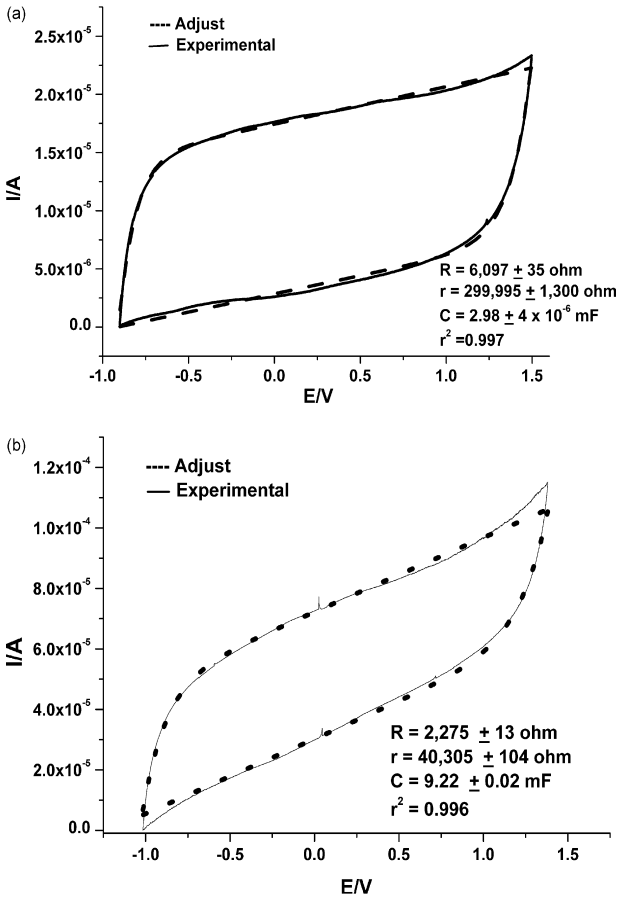

Fig. 5. Cyclic voltammograms after 20 cycles at 5 mV s^{-1} for the EDLCs with (a) 5 wt.% and (b) 10 wt.% of CB.

Cyclic voltammograms for the capacitors with 5 wt.% and 10 wt.% CB, at 5 mV s^{-1} and room temperature, presented in Fig. 5, show a deviation of the box-like shape typical of an ideal

Table 2
Main EDLC results for devices with 5 wt.% and 10 wt.% of nanostructured CB

	5 wt.% CB			10 wt.% CB		
	Impedance spectroscopy	Voltametry[a]	Chronocoulometry[b]	Impedance spectroscopy	Voltametry[a]	Chronocoulometry[b]
Capacitance (mF)	1.29	2.98	2.16	5.88	9.22	7.63
Specific capacitance[c] (F g^{-1})	2.38	5.52	4.00	11.1	17.4	14.3
Specific capacitance (F cm^{-3})[d]	0.081	0.187	0.153	0.368	0.572	0.477
Energy density (Wh kg^{-1})	–	–	2.22	–	–	8.0
Power density (W kg^{-1})	–	–	26.7	–	–	96.0

[a] VC between −1 V and 1.4 V.
[b] Under 2 V.
[c] Taken into account the CB black mass on the two nanocomposite electrodes.
[d] Average volume of EDLCs = 1.6×10^{-2} cm^3.

Table 3
Results of the EDLC capacitors based on polymer films

Authors	Active material	Electrolyte	Specific capacitance[a] ($F\,g^{-1}$)	Areal capacitance ($mF\,cm^{-2}$)
Furtado et al. [11][a]	Carbon black Black Pearls 2000 (10 wt.% in polymer electrolyte film)	$Polyurethane_8/LiClO_4$	8.4	4
Gu et al. [14]	Activated carbon ($1200\,m^2\,g^{-1}$) and 5 wt.% Lonza carbon (KS-6)	PVDF-HFP (25%) + PC_{10}-$EC_{10}/LiClO_4$	4.3	100
Staiti et al. [16]	65 wt.% Black Pearls 2000/5 wt.% graphite fibers + 30 wt.% Nafion	Nafion 1100 ionomer swelled membranes	13.2	175
Hashmi et al. [17]	Activated carbon fabric ($2000\,m^2\,g^{-1}$)	$PEO_9/LiCF_3SO_3$ plasticized with 50 wt.% PEG200	4	20
This work	Carbon black Black Pearls 2000 (10 wt.% in polymer electrolyte film)	$(PEO\text{-}NPPP)_{11}/LiClO_4$	17	6

[a] A better result was obtained with 20 wt.% CB in Ref. [11], however, to compare with the present work, the EDLC with 10 wt.% CB is reported.

double layer capacitor [7] and redox peaks were not clearly observed. The potential scanning was repeated 20 times and no significant change was verified. The CV curves discrepancy from a box-like shape is assigned to the internal resistance and carbon porosity, which produces a current dependence of potential [7,10]. The fitting of CV curves with Eq. (1) yields the capacitances presented in Table 2.

Chronocoulometric dynamical method was also employed to investigate the capacitors behavior. The charge/discharge curves did not show significant loss of charge, even after a 1000 cycles, suggesting a good electrochemical stability of the material (see Fig. 6), which can be attributed to the high mechanical cohesion of the interfaces and good electrochemical stability of the electrolyte [11]. Moreover, the devices present a symmetrical behavior in relation to the charge/discharge process. Tens of thousands cycle measurements would be recommended for electrochemical capacitors, however, the experiment, in its limitations, allows a first evaluation of the device's behavior. The capacitances determined by this method are presented in Table 2. From these values, the EDLC with 5 wt.% and 10 wt.% CB could store 2.2 $Wh\,kg^{-1}$ and 8.0 $Wh\,kg^{-1}$ of energy, respectively.

Table 2 allows us to compare both devices investigated in this work, i.e., with 5 wt.% and 10 wt.% of nanostructured CB. The voltametric results are considered the most reliable method to evaluate capacitance [10]. The capacitor with 10 wt.% CB presented high values of specific capacitance and energy density, which is most interesting taken into account that the electrical conductivity is quite small for both types of electrode composites. Table 1 shows that there is no increase in glass transition or decrease in crystallinity when the CB content changes from 5 wt.% to 10 wt.%. Furthermore, the AFM analysis showed that the particles have similar size distribution. Several parameters can interfere in the capacitance values such as carbon surface area, number and pore size, pore cavity to pore throat ratios and tortuosity. Therefore, was observed that despite twofold increase in the carbon content (from 5 wt.% to 10 wt.%) there was close to fourfold increase in capacitance. Larger dispersibility of CB in the 10 wt.% CB device could explain this result. However, to confirm this, further AFM images are required. Tortuosity, or the degree to which the CB particles or pores depart from a straight line, may also interfere in capacitance [44].

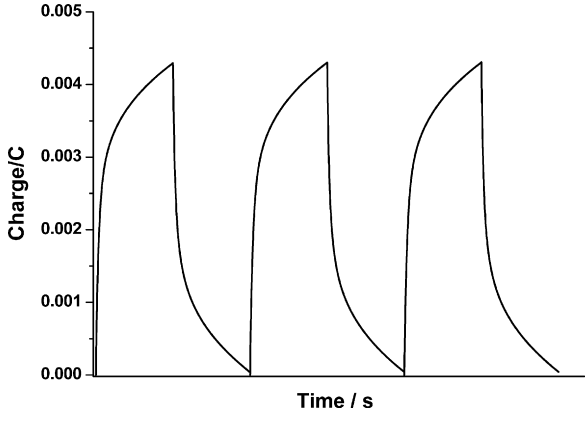

Fig. 6. Chronocoulometric curves of an EDLC with 5 wt.% of CB after 1000 cycles of charge–discharge—three last curves.

Finally, it is worthwhile to compare the results in this study with other reported studies. The context of comparison should be the EDLC prepared from solid polymer coatings or, at least, those using a polymer gel electrolyte, even considering that the plasticizer present in these systems are the main responsible for the ionic conductivity of the electrolytes and the wettability of carbon electrodes. Table 3 shows the areal capacitance of the device, which is largely influenced by the content of active material (carbon) in the electrode and the ionic access to the carbon surface, i.e., the porous properties and electrolyte characteristics. As the devices designed with disperse nanostructured CB in solid PE (this work and Ref. [11]) were studied with low content of CB, the value of capacitance by device area is low as expected. On the other hand, when the capacitance by weight is taken into account, the results for the totally solid EDLCs can be considered quite interesting. The value of 17 $F\,g^{-1}$ is stimulating taken into account all factors, which can be further exploited to enhance performance of this kind of capacitor.

4. Conclusion

An all solid polymeric capacitor was assembled using PEO-NPPP–$LiClO_4$ as solid polymer electrolyte and PEO-NPPP–CB as electrode material. NPPP is a triblock polyether of molar

mass 2000 g mol^{-1} and only 20 wt.% was added to high molar mass PEO. The spray coating technique allowed reproducible preparation of micrometric coatings of electrolyte and electrode, with the final device thickness being ∼130 μm. The 10 wt.% CB device presented a performance, assessed in specific capacitance (by total carbon mass), superior to other similar EDLCs reported in the literature, with a cyclability of more than 1000 cycles. The low content of active material used in the preparation of the electrode allowed a good dispersability and a nanostructured arrangement, whereas limiting the total capacitance delivered by the device. Nevertheless, the concept of a totally solid and plastic EDLC, without plasticizer and therefore without leakage problems, appears to provide an interesting alternative to be pursued.

Acknowledgments

This work was supported by Instituto do Milênio de Nanociências/PADCTIII/CNPq/MCT, CT Energia-2003-Supercapacitores. The authors are grateful to CNPq for scholarship of Rodrigo Lassarote Lavall, to professor Tulio Matencio (Departamento de Química/UFMG, Brazil) for the discussions and suggestions in the treatment of the electrochemical data and to the images provided by Laboratório de Microanálises/UFMG/CDTN/CNEN.

References

[1] R. Kötz, M. Carlen, Electrochim. Acta 45 (2000) 2483–2498.
[2] Y.-h. Lee, K.-h. An, J.-e. Yoo, US Patent 6,454,816 (2002).
[3] S.A. Hashmi, H.M. Upadhyaya, Solid State Ionics 152–153 (2002) 883–889.
[4] Ch. Emmenegger, Ph. Mauron, P. Sudan, P. Wenger, V. Hermann, R. Gallay, A. Züttel, J. Power Sources 124 (2003) 321–329.
[5] J.M. Pernaut, G. Goulart, J. Power Sources 55 (1995) 93–96.
[6] A.S. Aricò, P. Bruce, B. Scrosati, J.-M. Tarascon, W.V. Schalkwijk, Nat. Mater. 4 (2005) 366–377.
[7] E. Frackowiark, F. Béguin, Carbon 39 (2001) 937–950.
[8] E. Frackowiark, S. Delpeux, K. Jurewiczk, K. Szostak, D. Cazorla-Amoros, F. Béguin, Chem. Phys. Lett. 361 (2002) 35–41.
[9] A.G. Pandolfo, A.F. Hollenkamp, J. Power Sources 157 (2006) 11–27.
[10] J. Niu, W.G. Pell, B.E. Conway, J. Power Sources 156 (2006) 725–740.
[11] C.A. Furtado, P.P. de Souza, G.G. Silva, T. Matencio, J.M. Pernaut, Electrochim. Acta 46 (2001) 1629–1634.
[12] Y. Matsuda, M. Morita, M. Ishikawa, M. Ihara, J. Electrochem. Soc. 140 (1993) L109–L110.
[13] S. Sekido, Y. Ninomiya, Solid State Ionics 3–4 (1981) 153–156.
[14] H.-B. Gu, J.-U. Kim, H.-W. Song, G.-C. Park, B.-K. Park, Electrochim. Acta 45 (2000) 1533–1536.
[15] A. Lewandowski, M. Zajder, E. Frackowiark, F. Béguin, Electrochim. Acta 46 (2001) 2777–2780.
[16] P. Staiti, M. Minutoli, F. Lufrano, Electrochim. Acta 47 (2002) 2795–2800.
[17] S.A. Hashmi, R.J. Latham, R.G. Linford, W.S. Schlindwein, J. Chem. Soc. Faraday Trans. 92 (1997) 4177–4182.
[18] A. Lewandowski, M. Krzyzanowski, Electrochim. Acta 48 (2003) 1325–1329.
[19] M.B. Armand, in: J.R. Macllum, C.A. Vincent (Eds.), Polymer Electrolytes Reviews, vol. 1, Elsevier Applied Science, London, 1987, pp. 1–22.
[20] M.S. Mendolia, G.C. Farrington, in: L.V. Interrante, L.A. Caspar, A.B. Ellis (Eds.), Advances in Chemistry Series: Materials Chemistry an Emerging Discipline, ACS, Washington, 1995, pp. 107–129.
[21] I. Albinsson, B.E. Mellander, J.R. Stevens, J. Chem. Phys. 96 (1992) 681–690.
[22] D. Baril, C. Michot, M. Armand, Solid State Ionics 94 (1997) 35–47.
[23] J.J. Fontanella, J. Chem. Phys. 11 (1999) 7103–7109.
[24] M. Watanabe, M. Itoh, K. Sanui, N. Ogata, Macromolecules 20 (1987) 569–573.
[25] A. Killis, J.F. LeNest, A. Gandini, H. Cheradame, J.P. Cohen-Addad, Polym. Bull. 6 (1982) 351–358.
[26] M.A. Ratner, in: J.R. Macllum, C.A. Vincent (Eds.), Polymer Electrolytes Reviews, vol. 1, Elsevier Applied Science, London, 1987, pp. 173–236.
[27] J. Van Heumen, W. Wieczorek, M. Siekierski, J.R. Stevens, J. Phys. Chem. 99 (1995) 15142–15152.
[28] F.M. Gray, in: J.A. Connor (Ed.), RSC Materials Monographs, 1st ed., The Royal Society of Chemistry, Cambridge, 1997, p. 175.
[29] J.J. Fontanella, M.C. Wintersgill, J.J. Immel, J. Chem. Phys. 110 (1999) 5392–5402.
[30] C.A. Angell, Polymer 38 (1997) 6261–6266.
[31] K. Kinoshita, Carbon: Electrochemical and Physicochemical Properties, first ed., John Wiley & Sons, New York, 1988, pp. 1–85.
[32] J.-C. Huang, Adv. Polym. Technol. 21 (2002) 299–313.
[33] Y. Wan, C. Xiong, J. Yu, D. Wen, Compos. Sci. Technol. 65 (2005) 1769–1779.
[34] R.L. Lavall, J.P.C. Trigueiro, R.S. Borges, A.S. Ferlauto, C.A. Furtado, G.G. Silva, Macromol. Symp. 229 (2005) 160–167.
[35] R. Richner, S. Müller, A. Wokaun, Carbon 40 (2002) 307–314.
[36] N.L. Wu, S.Y. Wang, J. Power Sources 110 (2002) 233–236.
[37] C. Berthier, W. Gorecki, M. Miner, M.B. Armand, J.M. Chabagno, P. Rigaud, Solid State Ionics 11 (1983) 91–95.
[38] E. Quartarone, P. Mustarelli, A. Magistris, Solid State Ionics 110 (1998) 1–14.
[39] T. Hamaide, Eur. Polym. J. 30 (1994) 961–965.
[40] Y. Kato, K. Hasumi, S. Yokoyama, T. Yabe, H. Ikuta, Y. Uchimoto, M. Wakihara, J. Therm. Anal. Calorim. 69 (2002) 889–896.
[41] M.L. Williams, R.F. Landel, J.D. Ferry, J. Am. Chem. Soc. 77 (1955) 3701–3707.
[42] S. Tóth, M. Füle, M. Veres, J.R. Selman, D. Arcon, I. Pócsik, M. Koós, Thin Solid Films 482 (2005) 207–210.
[43] S.H. Munson-McGee, Phys. Rev. B 43 (1991) 3331–3336.
[44] H.P. Kamath, US Patent 6,714,402 (2004).